Quantification of Damage Evolution for a Micromechanical Model of Ductile Fracture in Spallation of Tantalum

A. Zurek, W. Thissell, D. Tonks, R. Hixson, F. Addessio

J. PHYS IV FRANCE 7 (1997)
Colloque C3, Supplément au Journal de Physique III d'août 1997

Quantification of Damage Evolution for a Micromechanical Model of Ductile Fracture in Spallation of Tantalum

A.K. Zurek, W.R. Thissell, D.L. Tonks*, R. Hixson** and F. Addessio***

Materials Research & Processing Science, Los Alamos National Laboratory, Los Alamos NM 87545, U.S.A.
** Nuclear Hydrodynamic Applications, Los Alamos National Laboratory, Los Alamos NM 87545, U.S.A.*
*** Detonation Science and Technology, Los Alamos National Laboratory, Los Alamos NM 87545, U.S.A.*
**** Fluid Dynamics, Los Alamos National Laboratory, Los Alamos NM 87545, U.S.A.*

Abstract. We present *quantification* of micromechanical features such as voids that comprise the ductile fracture obtained under uniaxial strain condition in a spall test of commercial purity tantalum. Two evolutionary parameters of ductile fracture void formation are quantified: (i) the void volume fraction (porosity) and its distribution with respect to the distance from the main spall fracture plane, and (ii) void diameter distribution. The results complement the discussion of the implications of void clustering and linking for micromechanical modeling of ductile fracture as presented in a paper by D. L. Tonks *et al.* in this volume.

Résumé. Nous présentons une *quantification* des caractéristiques micromécaniques décrivant la rupture ductile, tels les vides, en déformation uniaxiale obtenue lors d'un test d'écaillage sur du tantale de pureté commerciale. Nous décrivons l'évolution des vides jusqu'à la rupture par: (i) la fraction volumique de vide (porosité) et sa distribution en fonction de la distance par rapport au plan d'écaillage; et (ii) la distribution des diamètres des vides. Ces résultats complètent la discussion sur les implications de la coalescence des vides pour la modélisation micromécanique de la rupture ductile présentée par D.L. Tonks *et al.* lors de cette même conférence.

1. INTRODUCTION

Spallation is one of many experimental configurations that can produce controlled dynamic fracture for research purposes. Spallation is defined as a dynamic uniaxial strain fracture experiment. It occurs in a material due to tensile stresses generated by the interaction of two release (rarefaction) waves [1]. Ductile spallation is a process of damage accumulation and linkage which differs drastically from ductile fracture damage in the uniaxial tensile test by virtue of the stress state and the rate of damage accumalation. In the tensile test, voids are subject to a nearly uniaxial tensile stress field; homogeneous plastic strain dominates the flow process from the early stages. Due to the uniaxial deformation field the voids grow as elongated ellipsoids and the overall change in vicinity of failure is small, on the order of 5%[2]. In contrast, in ductile spallation, voids are subject to extremely high, nearly isotropic, triaxial, and very localized hydrostatic stress fields. Void growth and coalescence dominate all stages of the damage process to a porosity of up to about 30% at the principal spall plane. Voids assume nearly spherical shapes due to the isotropic triaxial stress field. The growth rate of voids is very high and the void distribution is dictated by the large gradient in stress generated by the interaction of release waves. Porosity, void formation, growth, and coalescence therefore, are important variables in descriptions of spallation and the fracture criteria of the material [1, 3, 4].

An impactor is launched at a stationary plate sample in a spallation plate impact experiment. Impact results in loading that induces a shock wave at the impact plane. The shock waves travel from the impact plane to the flyer plate back surface and the target back surface. Reflection of the waves occur at the free surfaces. The two release shock waves meet inside the sample to produce a region of tension. The sample will fail within this region and separate into two pieces if the amplitude of the tensile wave exceeds the spall strength of the material. Otherwise, the sample will develop an incipient deformation zone within this region with characteristic voids, cracks, and plastic deformation. In addition to the damage process the shock wave preceding spallation produces extensive shock hardening of the material and thus a reduction in the work hardening capacity.

The process of deformation and fracture can be investigated by using a "soft" sample recovery system and microscopic observation of the damage after the impact [1]. VISAR laser interferometry can be employed to record the back free surface velocity of the target [5, 6]. Both techniques were utilized in this study of spallation properties of commercial-purity tantalum subjected to a peak shock pressure just below

spallation. The reason for choosing this peak pressure was to obtain an incipient deformation zone to study evolving porosity, void formation and their distribution [7].

In this paper, two evolutionary parameters of ductile fracture void formation are quantified: (i) the porosity with respect to the distance from the main spall fracture plane and (ii) the statistical void diameter distribution. In a companion paper by D. L. Tonks *et al.* in this volume the implications of statistical void linking and coalescence to micromechanical modeling of ductile fracture are discussed.

A micromechanical model of spall is a theoretical analysis that attempts to explain, from more fundamental principles [8-11], the microscale interactions of voids which form complex fracture patterns (*e.g.*, Figure 1). Quantification of parameters in a micromechanical model, in combination with wave-propagation and spall calculations, should lead to an improved explanation of observed spall signals in materials undergoing void nucleation, growth and coalescence under dynamic loading conditions.

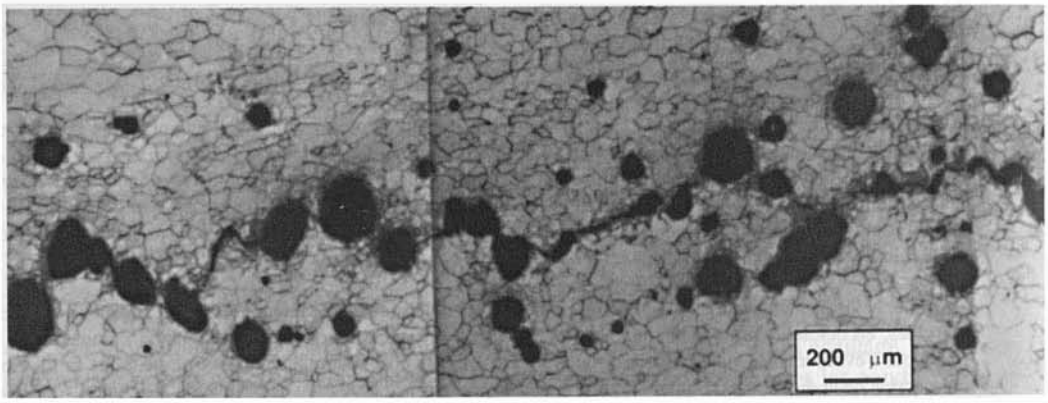

Figure 1: A fragment of ductile voids obtained in an incipient spall test of commercial purity tantalum (shock pressure ~7.0 GPa and shock duration 1 μs).

2. MATERIAL AND EXPERIMENT DESCRIPTION

In this study we used commercially pure (triple electron beam arc melted) unalloyed tantalum plate with a measured composition of 6 ppm carbon, 24 ppm nitrogen, 56 ppm oxygen, < 1 ppm hydrogen, 19 ppm iron, 25 ppm nickel, 9 ppm chromium, 41 ppm tungsten, 26 ppm niobium, and the balance tantalum. The tantalum plate was in an annealed condition and had an equiaxed grain structure of 68 mm grain size [12].

2.2 Spall Experiments

We performed uniaxial strain spall tests utilizing an 80-mm single-stage launcher and recovery techniques as previously described [1]. VISAR interferometry was used to record the free surface velocity of the samples [5, 6]. A number of previous reports have described shock compression and release in metals including tantalum [13-19]. Tantalum's mode of failure and hence, spall strength are known to be a function of shock amplitude. Previous recovery and non-recovery spall tests reported a 5.2 GPa spall strength for a 6 GPa shock amplitude, 7.3 GPa spall strength for a 9.5 GPa shock amplitude, and 3.0 to 4.5 GPa spall strength for a 15 GPa shock amplitude [7, 12, 20]. These spall strength values compare favorably with our results[21]. Tantalum samples for this investigation were spalled at ~7.0 GPa peak pressure and a 1 μs pulse duration under symmetric impact conditions in order to develop an incipient spall. Recovered spalled samples were analyzed using optical microscopy to characterize the fracture morphology.

2.3 Microscopy

The spall test of commercially pure tantalum performed at a ~7.0 GPa peak pressure developed an incipient spall. The cross section of the recovered, polished, and lightly etched [22] spall sample showed almost spherical voids running across the entire damaged area with multiple linking ranges connecting individual voids. Figure 1 shows a fragment of the cross section of the incipiently spalled sample used in the

following analysis. There are two salient feature of the micrograph: (a) the voids are spherical due to the magnitude of the hydrostatic stresses and (b) the degree of porosity is large because the damage process is localized due to the severe stress gradients and high strain rate.

2.4 Quantitative analysis

Qualitative analytical descriptions of ductile fracture in spall were sufficient for most research purposes in the past. However, emerging models which try to describe ductile fracture are in need of quantitative parameters that would accurately describe evolutionary processes occuring during spall deformation leading to fracture. At present, most of the quantitative measurements of the crucial parameters that characterize ductile fracture (voids, void distribution, void linking ranges *etc.*) are possible using computer hardware and software. These measurements however, still require major interaction, decision making, and some pattern recognition help from the operator. The method described below was developed to quantify the deformation obtained in a spall test of tantalum.

2.4.1 The two and three dimensional analysis

Image Pro® software was used for the two dimensional quantification of the voids of the spalled tantalum sample. The image acquisition system consists of a metallographic microscope fitted with a video camera connected to a computer through a frame grabber. Individual images were captured at 740x480 pixel resolution at 24 bits color. The analysis was performed on a montage of 10 image frames taken at 50x magnification which represent the entire sample cross section. The advantages of analyzing a montage over individual images are the great reduction of edge effects which are magnification dependent, and a number increase in analyzed features.

A WYKO RST-Plus®, an optical profilometry system, was used for depth measurements of individual voids. RST-Plus is an optical, non-contact, profilometry system that utilizes interferometric techniques [23]. The system consists of an optical microscope fitted with an interferometer, a video camera, and a computer control and acquisition system.

The Image Pro® software allows us to identify voids and measure their location, size, aspect ratio, and the average diameter. This information, when combined with the data from the optical profilometry system that measures the depth of individual voids, gives us the three dimensional representation of the voids at the planar cut through the spalled samples.

2.4.2 Assumptions and limitations

Figure 2 shows a schematic representation of a metallographic cut through the spalled sample. The circles in this figure represent a two dimensional view of perfectly spherical, three dimensional voids.

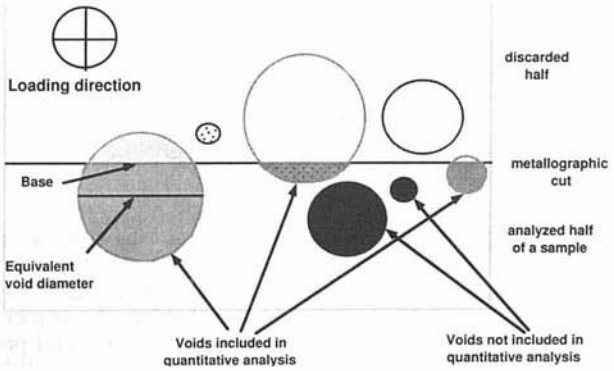

Figure 2: Schematic representation of a metallographic cut through the spalled sample. The circles in this figure represent the two dimensional view of the perfectly spherical, three dimensional voids.

The main assumption we are making in our analysis of the measured data is that the voids are perfectly spherical, however we are able to measure the aspect ratio of the voids. In addition, on the metallographically cut surface (perpendicular to the plane of Figure 2), only those cross sections of the voids will be visible that come in contact with the cut surface. Voids present below the surface, regardless of their size, will not be included in the surface count of the quantitative analysis. In our test, the void size and their distribution change with the distance from the principal spall plane. As a result, the quantified total porosity, which we define as the fraction of void area at a statistically representative cut through the spall plane, may not be equivalent to the total fraction of void volume in the analyzed spalled sample. The total fraction of void volume in fact will be underestimated. We are assuming in our porosity analysis that the void fractional area at a planar cut is representative of their volume fraction. This has been shown analytically to be valid for the case of randomly distributed spheres of uniform size [24]. However, the void sizes are not uniform, but have a distribution.

The depth measurement of a void (using a RST-Plus) allows us to calculate its equivalent void volume, by reevaluating the void diameter (the base of a sphere) based on the relationship between its measured void depth and its area measured at the metallographic cut (using Image Pro). Therefore, the availability of three dimensional probing of the voids (their surface area and a corresponding depth) is invaluable. The assessment of 3D volumetric damage from 2D images is a problem of considerable richness. There are early references to this problem [24]. This and many others are summed in the *Archive for History of Exact Sciences* [25], [26] and a more recent treatment is available in [27].

There are additional limitations of our measurement technique arising from the need to use several different software packages to acquire the data and the need of operator help in decision making and in pattern recognition during the data collection process. Therefore, the data collection process may become tedious and time consuming when a large data set is required for statistical analysis.

2.4.3 Analysis of the data.

Figure 3 shows the porosity as a function of the distance from the spall plane, where the spall plane is defined as the plane of maximum porosity.

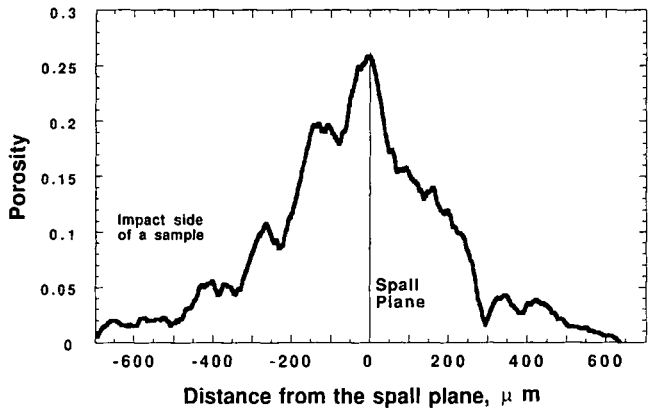

Figure 3: Change in porosity from the spall plane. Note the non-symmetrical porosity about the spall plane.

The porosity is defined here as a total void fractional area (the base of a spherical void) on the statistically random metallographic cut normal to the spall plane. There are several interesting findings resulting from this plot: (i) The porosity at the spall plane is about 0.26. This result is in excellent agreement with the previously measured and predicted condition for fracture in a spall test as expressed in terms of critical porosity. Ductile fracture in spallation is preceded by a large increase in porosity. In the case of copper the porosity was 0.30, at the fully spalled plane, as measured and predicted by [28] and [3], respectively. (ii) The porosity is not symmetrical with respect to the spall plane. When examining Figure 3, we observe secondary peaks of porosity appearing regularly, approximately every 135 μm, on the left side of the spall plane, which in our test corresponds to the projectile side of a sample. We believe that this is evidence of an interaction of the release wave (initiated from the free surfaces of the large void clusters evolving at the principal spall plane) with the rarefaction wave. Multiple spall layers have been observed in

metals subject to explosive loading [29, 30] and have been analyzed in terms of a dynamic void growth model [3]. However, the presence of periodic incipient spall planes in a flat-plate-impact recovery experiment, while a normal consequence of the coupling between void growth and wave propagation, is thought to be previously unobserved.

Figure 4(a) shows a distribution of the equivalent void diameters fitted to a log-normal density distribution function. From one metallographic cut, 322 voids, ranging in diameter from 14 μm to 389 μm were analyzed, and for graphing purposes all the data were consolidated into thirteen (13) - 25 microns wide bins. Figure 4(b) is a cumulative percentage probability graph of measured void diameters using the equivalent void diameter and the void diameter (base) as indicated by a two dimensional metallographic image. The equivalent void diameter is the diameter of a void which corresponds to the three dimensional sphere representing a void. Figure 2 defines the equivalent void diameter and the void base.

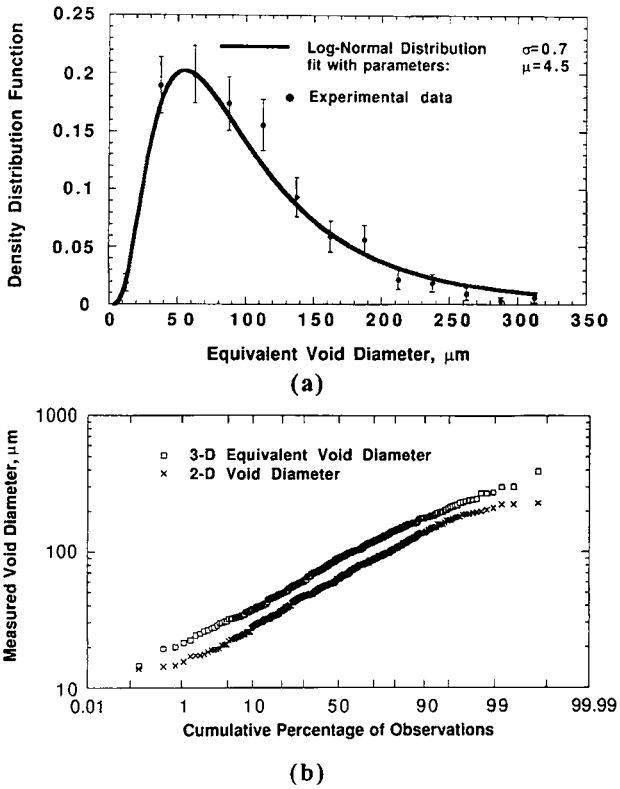

Figure 4: (a) Experimental data of the equivalent void diameter distribution fitted to the log-normal distribution function with parameters listed in the figure and χ^2/d.o.f. = 0.82. (b) Comparison of equivalent void diameter based on three dimensional void measurements to void diameters as measured from a two dimensional metallographic cut shown as a cumulative percentage probability plot.

Figure 4(b) indicates that the equivalent void diameters are significantly larger than the two dimensional (base) void diameter. Both diameter distributions are well described by a straight line in Figure 4(b) within the limits imposed by the measurement method and size of the data set and therefore indicate that a log-normal description of the data is appropriate. The equivalent void diameter at the distribution function maximum (mode) is about 58 μm in Fig. 4(a), while the median diameters are about 95 and 68 μm (Fig. 4 (b)) for the equivalent void diameter and base void diameter, respectively.

3. SUMMARY

The current work gives a quantitative analysis of the damage accumulation process related to spallation. The results show that the spatial distribution of stress state and strain rate in shock loading are reflected in both the void shape and the distribution of voids observed in spallation. There are secondary maxima in porosity

produced due to the complex reflection of the shock waves. The linkage of voids in the spall plane can be considered as the growth of damage in a highly shock hardened material under the action of high local triaxial stress. This results in localized linkage as discussed by [31]. It is significant to note that the local porosity levels achieved in spallation are much higher than in simple stress states such as uniaxial tension. This is because the values of the hydrostatic stress to flow stress ratio produce essentially local solid state cavitation processes rather than the distribution of extensive plastic strain which occurs in a conventional necking process. The important feature to be emphasized is that the quantitative assessment of both the level and the distribution of damage in spallation provides a method of linking experimental observations to existing models and to an eventually refinement of these models to encompass the physical description of variety of materials.

Acknowledgments

The authors want to thank Carl Trujillo for performing the spall test. David Embury and Jim Johnson are thanked for their comments and help in development of this project. This project is sponsored by the Joint DoD/ DOE Munitions Program.

References

[1] A. K. Zurek, J. N. Johnson, and C. E. Frantz, *Journal de Physique, 49*, C3, suppl. 9, (1988), 269.
[2] P. F. Thomason, *Ductile Fracture in Metals*, Pergamon Press, Oxford, 1990.
[3] J. N. Johnson, *J. of Applied Physics, 52*, 4, (1981), 2812.
[4] D. R. Curran, L. Seaman, and D. A. Shockey, *Physics Reports, 147*, (1987), 253.
[5] L. M. Barker and R. E. Hollenbach, *J. Applied Physics, 43*, 11, (1972), 4669.
[6] R. A. Graham and J. R. Asay, *High Temperature - High Pressure, 10*, (1978), 355.
[7] J. N. Johnson, R. S. Hixson, D. L. Tonks, *et al.*, in *Shock Compression of Condensed Matter*, edited by S. C. Schmidt and W. C. Tao (AIP, New York, 1995), p. 523.
[8] D. L. Tonks, A. K. Zurek, and W. R. Thissell, in *Metallurgical and Materials Applications of Shock-Wave and High-Strain-Rate Phenomena (EXPLOMET'95)*, edited by L. E. Murr, K. P. Staudhammer and M. A. Meyers (Elsevier, New York, 1995), p. 171.
[9] D. L. Tonks, *J. de Physique, IV*, C8, 4, (1994), 665.
[10] D. L. Tonks, in *Dynamic Plasticity and Structural Behaviors*, edited by S. Tanimura and A. S. Khan (Gordon and Breach, Luxembourg, 1995), p. 119.
[11] D. L. Tonks, in *High-Pressure Shock Compression of Solids II (Dynamic Fracture and Fragmentation)*, edited by L. Davison, D. E. Grady and M. Shahinpoor (Springer-Verlag, New York, 1995), p. 237.
[12] G. T. Gray, III, in *High-Pressure Science and Technology*, edited by S. C. Schmidt, J. W. Shaner, G. A. Samara and M. Ross (AIP, 1994), p. 1103.
[13] J. N. Johnson and P. S. Lomdahl, *J. de Physique, IV*, Colloque C3, (1991), 223.
[14] J. N. Johnson, P. S. Lomdahl, and J. M. Wills, *Acta Metallurgica, 39*, (1991), 3015.
[15] J. N. Johnson, R. S. Hixson, G. T. Gray, III, *et al.*, *J. of Applied Physics, 72*, (1992), 429.
[16] J. N. Johnson, in *High Pressure Shock Compression of Solids*, edited by J. R. Asay and M. Shahinpoor (Springer-Verlag, 1993), p. 217.
[17] J. N. Johnson, *J. of Physics and Chemistry of Solids, 54*, (1993), 691.
[18] J. N. Johnson, R. S. Hixson, D. L. Tonks, *et al.*, in *High Pressure Science and Technology-1993*, edited by S. C. Schmidt, J. W. Shaner, G. A. Samara and M. Ross (American Institute of Physics, 1993), Vol. 309, p. 1095.
[19] J. N. Johnson, in *High Pressure Science and Technology-1993*, edited by S. C. Schmidt, J. W. Shaner, G. A. Samara and M. Ross (American Institute of Physics, 1993), Vol. 309, p. 1145.
[20] G. T. Gray, III and A. D. Rollett, in *High Strain Rate Behavior of Refractory Metals and Alloys*, edited by R. Asfahani, E. Chen and A. Crowson (The Minerals, Metals and Materials Society, 1992), p. 303.
[21] A. K. Zurek, W. R. Thissell, J. N. Johnson, *et al.*, *Journal of Materials Processing Technology, 60*, (1996), 261.
[22] A. M. Kelly, S. R. Bingert, and R. D. Reiswig, *Microstructural Science, 23*, (1996), 185.
[23] P. J. Caber, S. J. Martinek, and R. J. Niemann, in *Proceedings of SPIE*, edited by , 1993), Vol. , p. 2088.
[24] B. Cavalieri, *Geometria Planara*, 1653.
[25] K. Andersen, *Archive for History of Exact Sciences, 31*, 4, (1985), 291.
[26] A. A. Glagolev, *Geometrical Methods*, 1933.
[27] H. E. Exner, in *Physical Metallurgy*, edited by R. W. Cahn and P. Haasen (North-Holland, New York, 1996), Vol. II, p. 944.
[28] L. Seaman, T. W. Barbee Jr., and D. R. Curran, (Stanford Research Institute of Technology, 1971).
[29] C. L. Mader, T. R. Neal, and R. D. Dick, (University of California Press, Berkeley, 1980).
[30] J. S. Rinehart, *J. Appl. Phys., 23*, (1952), 1229.
[31] P. F. Thomason, in *Recent Advances in Fracture*, edited by R. K. Mahidhara, A. B. Geltmacher, P. Matic and K. Sadananda (The Minerals, Metals and Materials Society, Warrendale, Pennsylvania, 1997).